

## Optical coherence tomography of the living human kidney

Peter M. Andrews\*, Hsing-Wen Wang<sup>†</sup>, Jeremiah Wierwille<sup>†</sup>, Wei Gong<sup>†,‡</sup>,  
Jennifer Verbese<sup>§</sup>, Matthew Cooper<sup>§</sup> and Yu Chen<sup>†,¶</sup>

\*Department of Biochemistry, Molecular and Cellular Biology  
Georgetown University Medical Center  
Washington, DC 20007, USA

<sup>†</sup>Fischell Department of Bioengineering, University of Maryland  
College Park, MD 20742, USA

<sup>‡</sup>College of Photonic and Electric Engineering  
Fujian Normal University, Fuzhou, China

<sup>§</sup>Medstar Georgetown Transplant Institute  
Georgetown University Medical Center  
Washington, DC 20007, USA

<sup>¶</sup>yuchen@umd.edu

Received 29 July 2013

Accepted 8 October 2013

Published 10 December 2013

*This manuscript is dedicated to the JIOHS Special Issue on Honoring the 100th Birthday of Professor Britton Chance.*

Acute tubular necrosis (ATN) induced by ischemia is the most common insult to donor kidneys destined for transplantation. ATN results from swelling and subsequent damage to cells lining the kidney tubules. In this study, we demonstrate the capability of optical coherence tomography (OCT) to image the renal microstructures of living human donor kidneys and potentially provide a measure to determine the extent of ATN. We also found that Doppler-based OCT (i.e., DOCT) reveals renal blood flow dynamics that is another major factor which could relate to post-transplant renal function. All OCT/DOCT observations were performed in a noninvasive, sterile and timely manner on intact human kidneys both prior to (*ex vivo*) and following (*in vivo*) their transplantation. Our results indicate that this imaging model provides transplant surgeons with an objective visualization of the transplant kidneys prior and immediately post transplantation.

**Keywords:** Optical coherence tomography; doppler optical coherence tomography; acute tubular necrosis; kidney transplantation; uriniferous tubules; glomerulus; renal blood flow.

## 1. Introduction

Acute tubular necrosis (ATN), caused by a lack of oxygen to the kidney (ischemia of the kidneys), is one of the most common causes of kidney failure. It is also a critical factor in determining the status of a kidney destined for transplantation. Previously it has been shown that noninvasive imaging techniques [i.e., tandem scanning confocal microscopy (TSCM)] could be used to determine the degree of ATN by analyzing the superficial nephrons of living rabbit kidneys and that these observations correlate with post-transplant renal function.<sup>1</sup> This is not surprising in that the status of superficial proximal convoluted tubules is indicative of the status of proximal convoluted throughout the entire kidney cortex. Noninvasive microscopic techniques are necessary for this determination because the biopsies required for conventional microscopy result in artifacts that are difficult to distinguish from ATN.<sup>2</sup> Unfortunately, the maximum penetration depth of TSCM is very limited (about 100  $\mu\text{m}$ ), which makes it difficult to nondestructively image the human kidney, especially when surrounded by an intact human renal capsule. Therefore, a non-invasive microscopic procedure that has enough penetrating ability to image the human kidney parenchyma and determine the extent of ATN would provide invaluable clinical information regarding kidney function.

Conventional noninvasive medical imaging modalities such as computerized tomography (CT), magnetic resonance imaging (MRI), ultrasound (US), single photon emission computerized tomography (SPECT) and positron emission tomography (PET) provide morphological and functional imaging with sub-millimeter to one-millimeter resolution (by MRI or US) or with several millimeter resolution (by PET). In terms of kidney functional imaging, nuclear scan, PET, MRI and US permit the measurement of renal blood flow (RBF). These techniques allow a wide-field-of-view imaging for entire single- or dual-kidney monitoring and evaluation. However, nuclear scan, PET and MRI imaging are limited by their cost, widespread availability, and the difficulty to be used at the bedside or during surgery. Contrast-enhancement US<sup>3,4</sup> is the only technique to receive significant attention in recent years as a possible post-operation (e.g., transplantation) imaging modality to monitor kidney perfusion.

Optical coherence tomography (OCT) can provide subsurface imaging of biological tissues with penetration depth at approximately 1 to 2 mm, and therefore, it can function as an “optical biopsy” to image kidney structure and function with a field-of-view (FOV) comparable to that of standard excisional biopsy and histology.<sup>5–7</sup> Subsurface imaging with OCT is similar to US but has significantly higher resolution (5–10 times) than clinical US, providing depth-resolved imaging of tissue microstructure with micron-level resolution near that of histology. The advantage is that OCT imaging can be performed in real time without the removal of a tissue specimen (i.e., biopsy) for staining and subsequent histological analysis. OCT has already been successfully translated to various clinical applications including ophthalmology,<sup>8</sup> cardiology,<sup>9</sup> gastroenterology,<sup>10–13</sup> urology,<sup>14,15</sup> and gynecology,<sup>16</sup> among others. In a recent study of *in vivo* OCT human kidney, the OCT signal attenuation was used to differentiate malignant tissues from normal.<sup>17</sup> However, clinical OCT imaging of the kidney is still an under-explored area with strong translational potential.

In addition, OCT can detect blood flow *in vivo* using the Doppler. Studies have shown the feasibility of quantifying blood flow *in vivo* in the human retina,<sup>18–24</sup> skin,<sup>25–27</sup> brain,<sup>28,29</sup> and gastrointestinal tract,<sup>30,31</sup> as well as other locations. Doppler OCT (DOCT) combines the ability of OCT to capture high-resolution structural images with corresponding Doppler velocity maps that can be merged together to identify regions with moving reflectors, indicating blood flow. Thus, OCT/DOCT is a powerful tool that combines structural and functional imaging which could be used to evaluate kidney status *in vivo* and in real time during and following surgical procedures.

In this study, we demonstrate the ability of OCT/DOCT to diagnose ATN in human donor kidneys both prior to and following their transplantation. Our OCT/DOCT images show the morphological and functional information of renal cell swelling, tubular spatial distribution and glomerular blood flow.

## 2. Material and Methods

### 2.1. OCT System setup and design

A custom-built OCT system with a fiber-optic, hand-held probe was used in this study, enabling

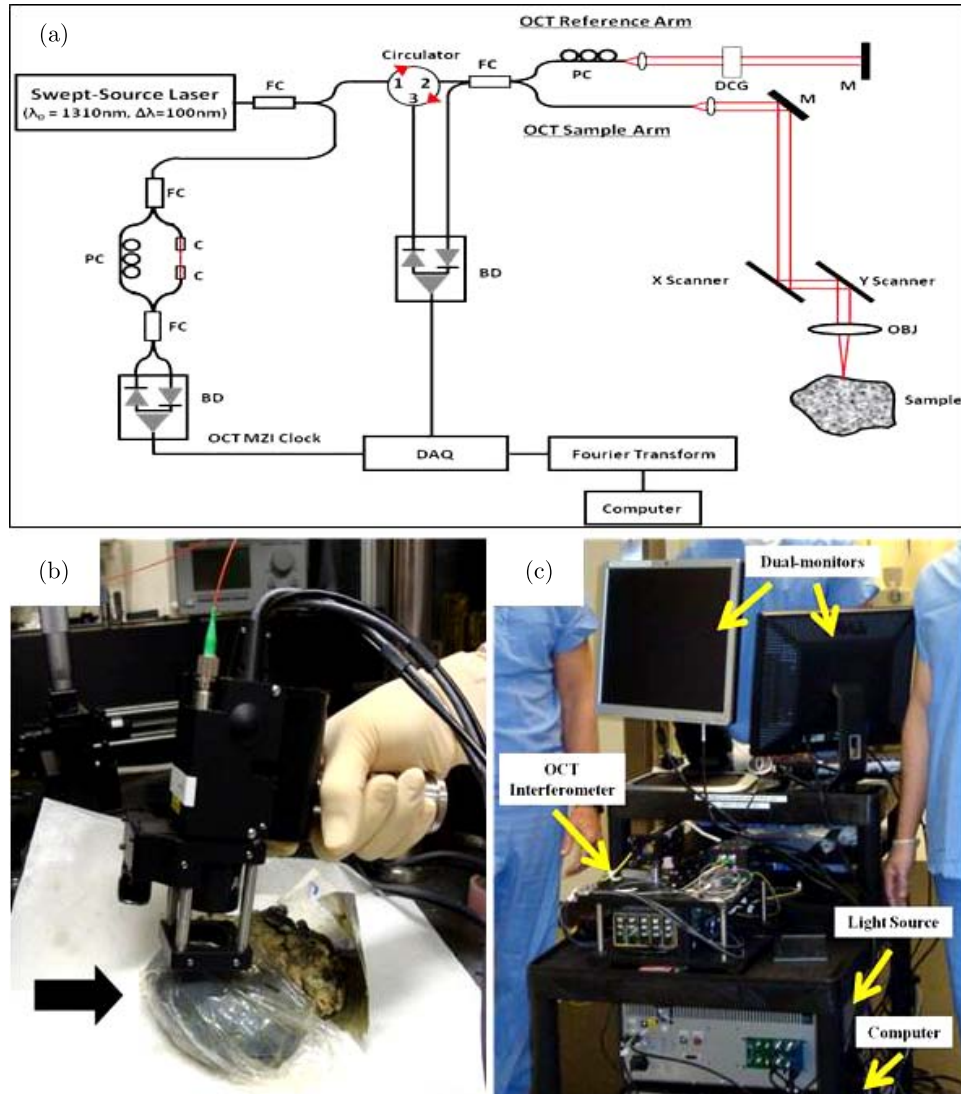


Fig. 1. (a) Schematics of hand-held OCT imaging probe for intra-operative kidney imaging. FC; fiber coupler, PC: polarization controller, C: collimator, MZI: Mach-Zehnder interferometer. M: mirror, BD: balanced detector, DAQ: data acquisition board. DCG: dispersion compensating glasses, OBJ: objective. (b) A close look of OCT hand-held probe. (c) Portable hand-held OCT imaging system setup for clinical imaging during kidney transplantation. Dual-monitor output allows for simultaneous viewing by the physicians for evaluation and probe positioning and for our team for data collection.

real-time, intra-operative OCT imaging during kidney transplant procedures [see Fig. 1(a)]. Briefly, the details of the OCT system used in this study consisted of a Fourier-domain OCT system with swept-source laser operating at 1310-nm center wavelength and 100-nm bandwidth with  $\sim 90$  dB sensitivity. The OCT axial resolution was  $\sim 12 \mu\text{m}$ , and using a 2.0x objective in the sample arm, a transverse resolution of  $\sim 15 \mu\text{m}$  was achieved as determined by resolution chart. Wavelength sweeping frequency was 16 kHz enabling real-time 2D imaging. OCT image pixel dimensions were as follows: 1024 [X] by 512 [Z], and associated

2D image scan dimensions were 3.75 mm [X] by 2.0 mm [Z].

Figure 1(b) shows the hand-held OCT imaging probe being used to image a fixed (i.e., preserved) kidney *ex vivo*. For operating room (OR) imaging, the hand-held OCT imaging device was assembled on a portable cart that can be easily wheeled into and out of the OR. Figure 1(c) shows the portable imaging system on the three-level utility cart that was used to house and transport the system to the OR. The imaging system was equipped with two output monitors facing opposing directions. One monitor enabled the operator to visualize and

record the data while the second monitor let the physicians visualize the imaging in real time.

## 2.2. Transplant patients and data collection

Prior to engaging in this research, the protocol was approved by the Institutional Review Boards at both Georgetown University and the University of Maryland College Park. Patients scheduled to receive kidney transplant at Georgetown University Medical Center (Georgetown, Washington DC) were enrolled in this study. Informed consent was obtained from all patients prior to imaging. A total of 29 patients enrolled in this study (mean donor age of 47 years), and for each patient we imaged the kidney prior to transplant (i.e., *ex vivo*) and also following transplantation and reperfusion (i.e., *in vivo*).

Following procurement from the donor, the kidney was transferred to a sterile ice bath solution prior to its transplantation. During this time, the kidney was imaged using our hand-held OCT imaging probe (*ex vivo* kidney). The entire hand-held probe with its six-foot length of cords was covered with a sterile camera sleeve. A 1.5-cm circular hole was cut in the end of the

sleeve and covered with a commercially available, sterile, transparent “Tegaderm” film (3M Health Care, St. Paul MN). This setup provided a sterile and moisture barrier without impeding the imaging laser beam. It took about 2–5 min to image the entire kidney *ex vivo*. Following transplantation of the kidney into the patient and re-establishment of blood flow to the donor kidney, we imaged the transplanted kidney again (*in vivo* kidney). For *in vivo* kidney imaging, the interference fringe data (the complex OCT signal including both magnitude and phase information) was recorded to enable DOCT processing and analysis. Again, the time for surveying the transplant kidney was 2–5 min.

## 3. Results

### 3.1. *Ex vivo* kidney imaging

While in a sterile ice bath prior to transplantation into the recipient, the entire donor kidney surface was surveyed by OCT (i.e., surveyed globally). Figure 2 shows representative OCT imaging of the *ex vivo* kidney prior to transplantation. The kidney parenchyma containing uriniferous tubules, glomeruli and blood vessels are visible beneath the

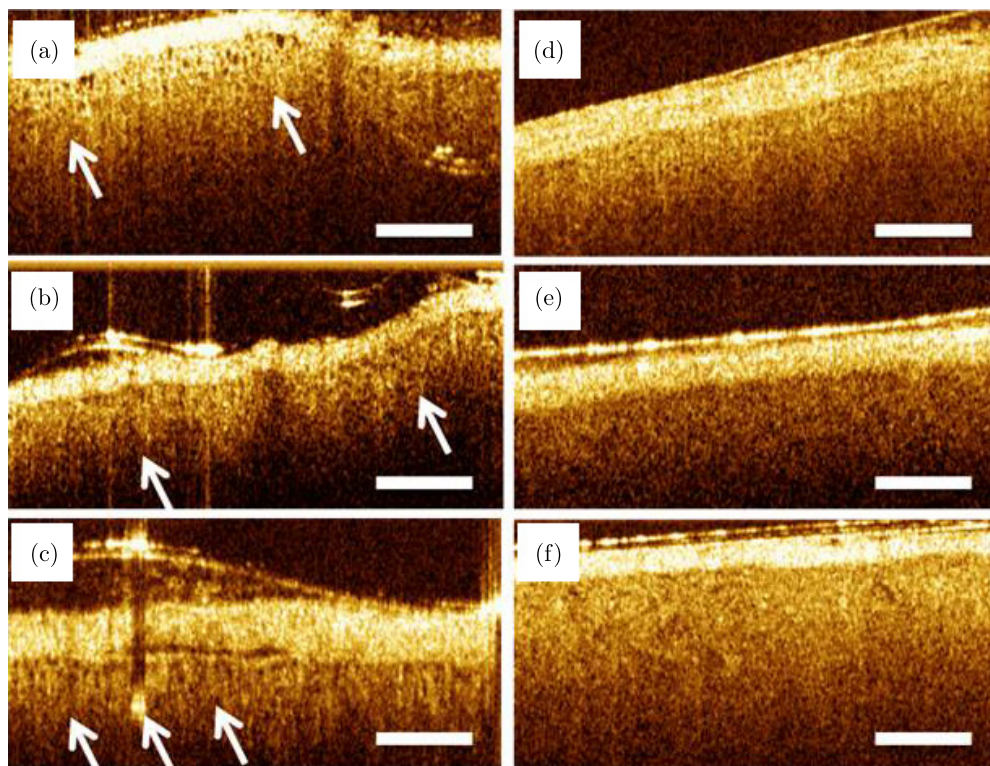


Fig. 2. *Ex vivo* OCT imaging of human donor kidney. Each is a representative OCT image from different human subject (a)–(c) shows opening tubules (see arrows), while in (d)–(f), most of the tubules are closed. Scale bar = 500  $\mu\text{m}$ .

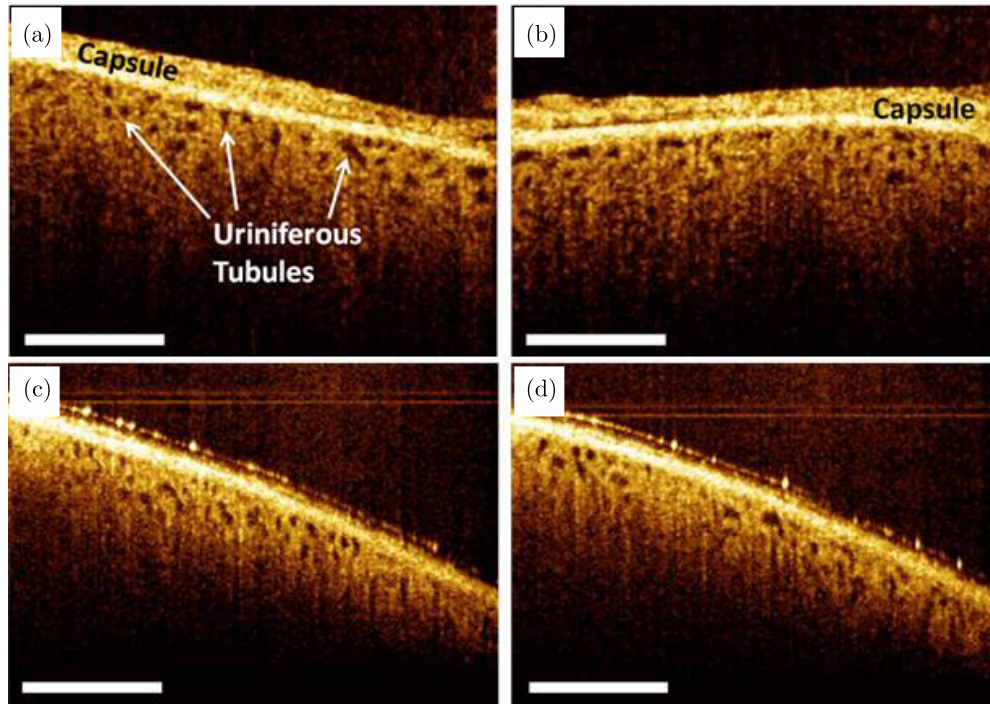


Fig. 3. OCT imaging of human kidneys following transplantation showing open uriniferous tubules below the renal capsule in two different patients ((a) and (b) are for one patient and (c) and (d) are for another). Tubules appear to be fairly open and round with some degree of homogeneity throughout the images. Scale bar = 500  $\mu\text{m}$ .

intact kidney capsule. Most important were significant variations in the openness of lumens of the proximal convoluted tubules (see Fig. 2). An analysis of post-transplant function revealed that this decrease in the proximal convoluted tubule luminal diameters correlated closely with a poorer post-transplant renal function as measured by serum creatinine and blood urea nitrogen (BUN) values.

### 3.2. *In vivo* OCT kidney imaging

Following transplanting and re-establishing blood flow to the donor kidney, we performed OCT/DOCT imaging of the kidney within the abdominal cavity of

the patient (see Figs. 3 to 6). Figure 3 depicts representative *in vivo* kidney OCT images from two patients [Fig. 3(a) and 3(b) are from one, 3(c) and 3(d) are from another] showing cross-sectional profiles of superficial proximal tubules below the renal capsule. The openness of tubule lumens labeled in Fig. 3 reflects a functioning post-transplanted kidney. The poorest post-transplant function was seen in one patient who had suffered an additional normothermic ischemic insult during reimplantation. This patient's transplanted kidney did not show open tubules that correlated with very poor post-transplant renal function.

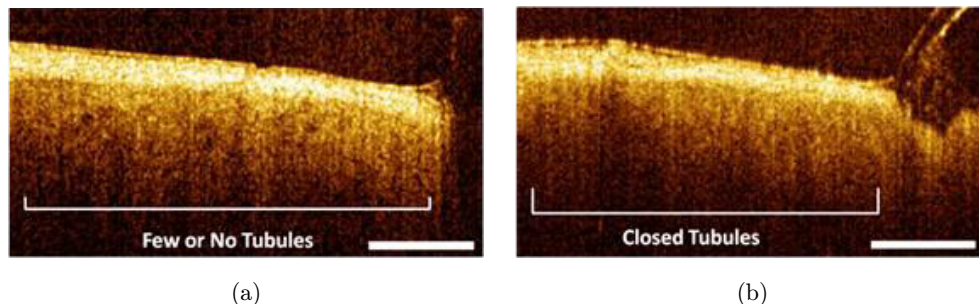


Fig. 4. Examples of a variation of *in vivo* OCT images of human kidney for tubule size/shape and tubule density/uniformity. tubule size/shape: (b) poor (d) moderate (f) good. Tubule density/uniformity: (a) poor (c) moderate (e) good. Scale bar = 500  $\mu\text{m}$ .

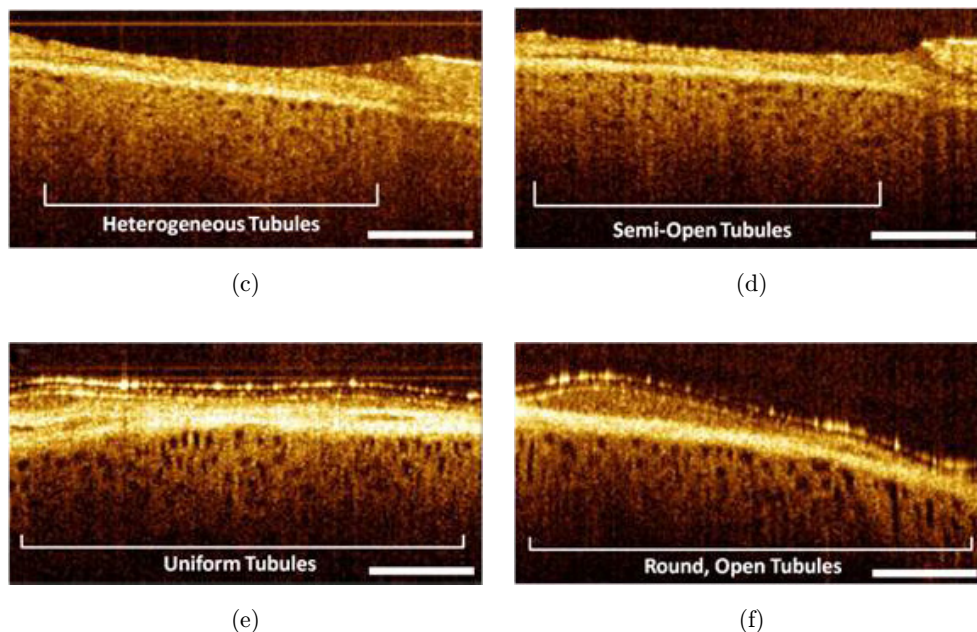


Fig. 4. (Continued)

The spatial distribution of opening tubule lumens exhibited variation from patient to patient. Example images of the variation of tubule morphology for both the size/shape and the density/

uniformity are evident in Fig. 4. Tubule size/ shape was grouped to three categories namely poor, moderate and good. Tubule density/uniformity was also grouped to poor, moderate and good categories.

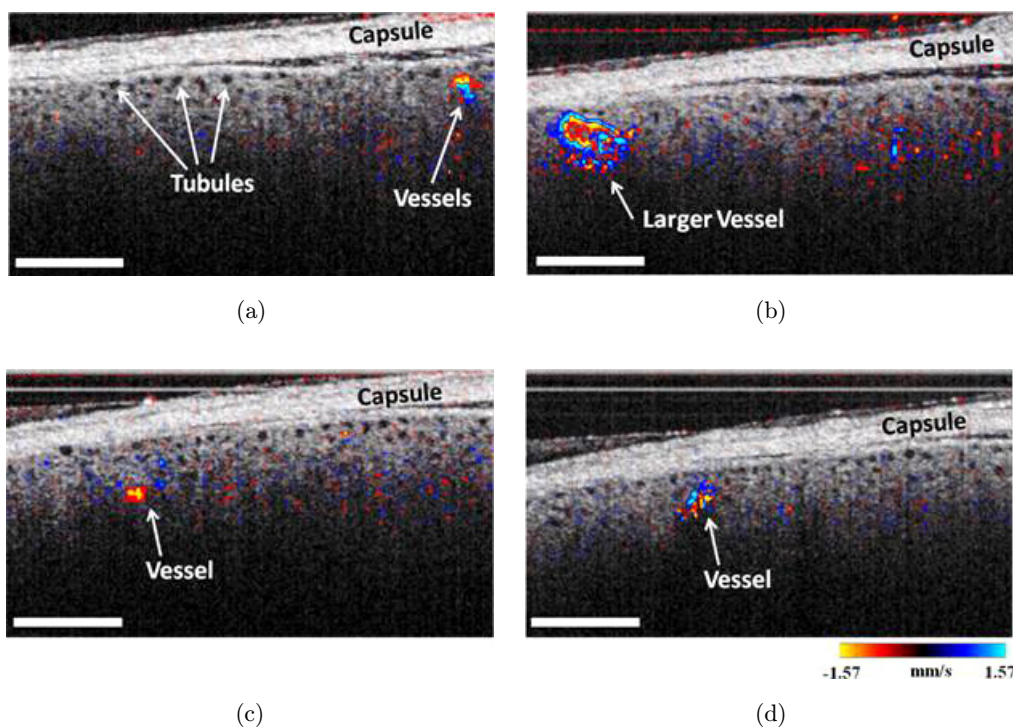


Fig. 5. *In vivo* human kidney showing open tubules and conical blood flow. Open tubules appear round and relatively uniform across all images. Also, a larger blood vessel is seen in (b) against some smaller vessels observed in (a), (c) and (d). Data are from a single patient. Scale bar = 500  $\mu\text{m}$ .

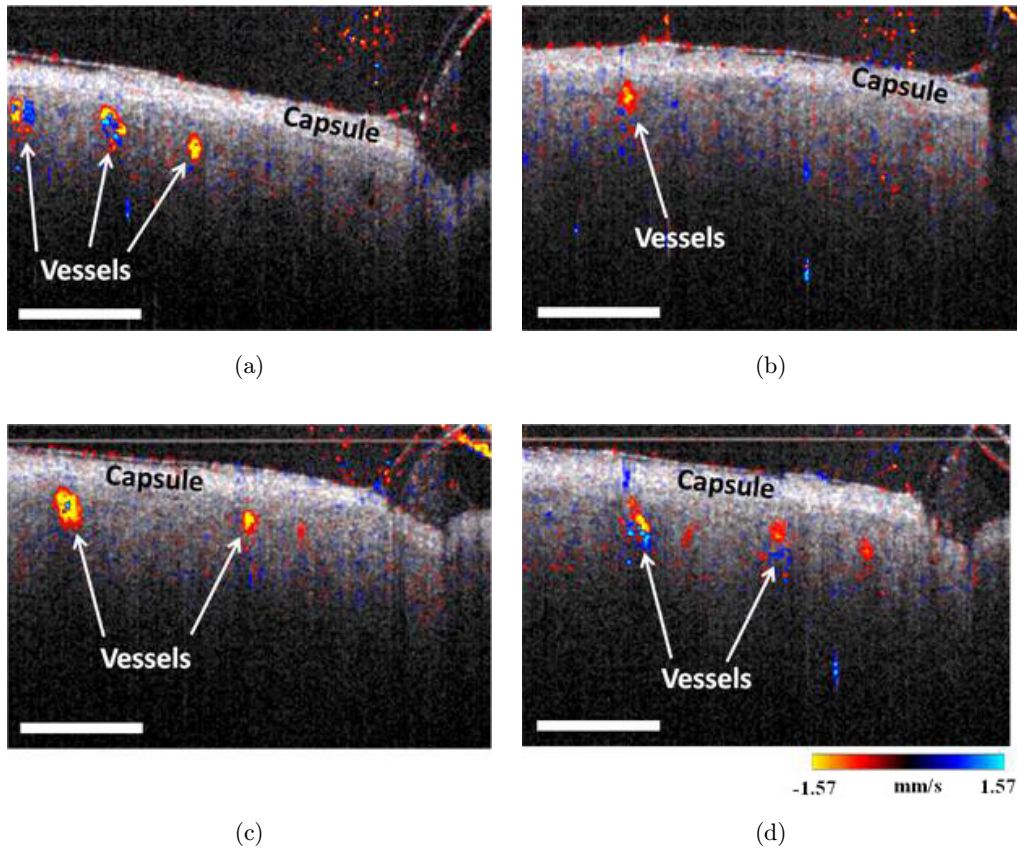


Fig. 6. OCT/DOCT imaging of *in vivo* kidney. Blood flow is seen in numerous cortical vessels but uriniferous tubules appear to be closed and not visible in adjacent image regions. Data are from another patient different from that shown in Fig. 4. Scale bar = 500  $\mu\text{m}$ .

These images illustrate the visual appearance represented by the various scoring values and can be used for standardizing the scoring system across multiple users for further analysis of tubule opening quantification following transplantation.

### 3.3. *In vivo* OCT/DOCT images show blood flow information together with tubular morphology

OCT fringe data were also recorded during *in vivo* imaging to enable DOCT imaging for visualizing blood flow in real time as shown in Figs. 5 and 6. OCT is displayed in grayscale and DOCT is overlaid with a color map. Blue-cyan represents blood flow in one direction while red-yellow represent blood flow in the opposite direction. Figure 5 shows the combination of morphological imaging with OCT and functional imaging with DOCT for one patient that displayed good tubular morphology and blood flow. Fairly densely packed uriniferous

tubules are observed with several cortical blood vessels indicating perfusion. The size of blood vessels varied from less than 100  $\mu\text{m}$  [see Fig. 5(c)] to more than 400  $\mu\text{m}$  [see Fig. 5(b)]. Figure 6 demonstrates the representative OCT/DOCT imaging of the transplant kidney *in vivo* from a different patient. While several vessels are noticed in Figs. 6(a)–6(d), no open tubules are observed around the vessels.

## 4. Discussion

This study demonstrates the use of OCT/DOCT imaging to evaluate the human kidneys prior to and following their transplantation. These preliminary results suggest that OCT/DOCT can provide novel and vital intra-operative monitoring and evaluation of the transplant kidney for predicting post-renal function. However, higher patient numbers are needed to provide additional correlative quantitative data. Also, in addition to semi-quantitative

image analysis, computing the average tubular diameter and tubular volume ratio (ratio of tubular volume per volume of parenchyma) would be a more objective measure to rank the morphological parameters of the OCT data. The OCT signal attenuation has been used for the determination of malignant tissues<sup>17</sup> and may possibly reflect kidney ischemic condition as well. However, Beer–Lambert law based on single-layer algorithm (which assumes homogenous tissue structures) might not work reliably on the heterogeneous OCT images we obtained. A more sophisticated algorithm needs to be developed to separate the scattering from capsule layer and subcapsular parenchyma, as well as to account for the effects of nonscattering open tubular regions. Those efforts will be pursued in the future together with the image analysis-based quantitative image parameter development.

In the present study, 3D imaging was not undertaken due artifacts associated with movement. Performing 3D OCT/DOCT imaging, however, would allow for more versatile metrics to be employed to quantify the image results, such as quantifying blood flow. However, 3D imaging is possible using newer laser systems that run at 100 kHz based on the micro-electro-mechanical system (MEMS)-tunable vertical cavity surface emitting laser (VCSEL) technology.<sup>32</sup> This MEMS-VCSEL OCT system provides high-speed imaging at 5 times faster than our currently available 16-kHz SS-OCT system. 3D OCT volumes with  $256 \times 256 \times 512$  pixels can be acquired approximately in 0.6 s, thereby dramatically reducing the motion artifacts. Furthermore, using novel laser sources, some studies report being able to perform scan rates reaching even 5 MHz.<sup>33</sup> At this scan rate it would take only 52 ms to perform a 3D scan consisting of 262,144 axial scans (XY:  $512 \times 512$ ). Higher scanning rates would decrease motion artifacts during image acquisition and also enable faster blood velocities to be detected with DOCT. In addition, higher resolution might also help to enhance the classification of imaging parameters to predict transplant outcome.<sup>34</sup>

Recent studies have shown dramatic difference in renal microvascular blood flow (blood cell velocities) between grafts from deceased donors versus living donors.<sup>35,36</sup> Since post-graft function has already been demonstrated to correlate with the openness of proximal kidney tubules and ischemic insult in rabbit studies,<sup>2</sup> a clinical trial that

investigates this technique in humans for living donors versus deceased donors would yield promising insights into the correlation between the duration of ischemic injury and post-graft function. The present study focused solely on living donors that had a relatively short duration of ischemic injury. Therefore, the results suggest that it is a suitable image modality to investigate the longer ischemic times associated with donor kidneys from cadavers as well. Our preliminary correlation studies of OCT images with post-transplant kidney function indicated donor kidneys with patent tubule lumens both prior to and following revascularization had the best post-transplant renal function.<sup>37</sup> More studies are needed to determine the ultimate clinical utilities of OCT in determining the status of donor kidney.

In conclusion, OCT is a powerful medical imaging technology that can reveal microstructure and blood flow in biological tissue in real time. Our preliminary results demonstrate that OCT is a safe, noninvasive procedure that can assess donor kidney status in a timely fashion in the OR and provide important information that can be used to predict post-transplant kidney function.

## Acknowledgments

We acknowledged medical students, Mr. Daniel Joh, Peter Alexandrov, Derek Rogalsky, Patrick Moody and Allen Chen for their assistant at operating room. We also thank Dr. James Jiang and Alex Cable from Thorlabs Inc. for technical support.

## References

1. P. M. Andrews, B. S. Khirabadi, B. C. Bengs, "Using tandem scanning confocal microscopy to predict the status of donor kidneys," *Nephron* **91** (1), 148–155 (2002).
2. A. B. Maunsbach, "The influence of different fixatives and fixation methods on the ultrastructure of rat kidney proximal tubule cells. I. Comparison of different perfusion fixation methods and of glutaraldehyde, formaldehyde and osmium tetroxide fixatives," *J. Ultrastruct Res.* **15**(3), 242–282 (1966).
3. K. Kalantarina, J. T. Belcik, J. T. Patrie, K. Wei, "Real-time measurement of renal blood flow in healthy subjects using contrast-enhanced ultrasound," *Am. J. Physiol. Renal Physiol.* **297**(4), F1129–F1134 (2009).

4. D. H. Kay, M. Mazonakis, C. Geddes, G. Baxter, "Ultrasonic microbubble contrast agents and the transplant kidney," *Clin. Radiol.* **64**(11), 1081–1087 (2009).
5. D. Huang, E. A. Swanson, C. P. Lin, J. S. Schuman, W. G. Stinson, W. Chang, M. R. Hee, T. Flotte, K. Gregory, C. A. Puliafito, J. G. Fujimoto, "Optical coherence tomography," *Science* **254** (5035), 1178–1181 (1991).
6. J. G. Fujimoto, "Optical coherence tomography for ultrahigh resolution in vivo imaging," *Nat. Biotechnol.* **21**(11), 1361–1367 (2003).
7. B. E. Bouma, S. H. Yun, B. J. Vakoc, M. J. Suter, G. J. Tearney, "Fourier-domain optical coherence tomography: Recent advances toward clinical utility," *Curr. Opin. Biotechnol.* **20**(1), 111–118 (2009).
8. J. S. Schuman, C. A. Puliafito, J. G. Fujimoto, *Optical Coherence Tomography of Ocular Diseases*, 2nd Edition, NJ Slack Inc. Thorofare. (2004).
9. I. K. Jang, B. Bouma, B. MacNeill, M. Takano, M. Shishkov, N. Iftima, G. J. Tearney, "In-vivo coronary plaque characteristics in patients with various clinical presentations using optical coherence tomography," *Circulation* **108**(17), 373–373 (2003).
10. B. E. Bouma, G. J. Tearney, C. C. Compton, N. S. Nishioka, "High-resolution imaging of the human esophagus and stomach in vivo using optical coherence tomography," *Gastrointest. Endosc.* **51**, 467–474 (2000).
11. M. V. Sivak, Jr., K. Kobayashi, J. A. Izatt, A. M. Rollins, R. Ung-Runyawee, A. Chak, R. C. Wong, G. A. Isenberg, J. Willis, "High-resolution endoscopic imaging of the GI tract using optical coherence tomography," *Gastrointest. Endosc.* **51**, 474–479 (2000).
12. X. D. Li, S. A. Boppart, J. Van Dam, H. Mashimo, M. Mutinga, W. Drexler, M. Klein, C. Pitris, M. L. Krinsky, M. E. Brezinski, J. G. Fujimoto, "Optical coherence tomography: Advanced technology for the endoscopic imaging of Barrett's esophagus," *Endoscopy* **32**(12), 921–930 (2000).
13. Y. Chen, A. D. Aguirre, P. L. Hsiung, S. Desai, P. R. Herz, M. Pedrosa, Q. Huang, M. Figueiredo, S. W. Huang, A. Koski, J. M. Schmitt, J. G. Fujimoto, H. Mashimo, "Ultrahigh resolution optical coherence tomography of Barrett's esophagus: Preliminary descriptive clinical study correlating images with histology," *Endoscopy* **39**(7), 599–605 (2007).
14. A. V. D'Amico, M. Weinstein, X. Li, J. P. Richie, J. Fujimoto, "Optical coherence tomography as a method for identifying benign and malignant microscopic structures in the prostate gland," *Urology* **55**(5), 783–787 (2000).
15. Z. Wang, C. S. Lee, W. C. Waltzer, J. Liu, H. Xie, Z. Yuan, Y. Pan, "In vivo bladder imaging with microelectromechanical-systems-based endoscopic spectral domain optical coherence tomography," *J. Biomed. Opt.* **12**(3), 034009 (2007).
16. C. Pitris, A. Goodman, S. A. Boppart, J. J. Libus, J. G. Fujimoto, M. E. Brezinski, "High-resolution imaging of gynecologic neoplasms using optical coherence tomography," *Obstet. Gynecol.* **93**(1), 135–139 (1999).
17. K. Barwari, D. M. de Bruin, D. J. Faber, T. G. van Leeuwen, J. J. de la Rosette, M. P. Laguna, "Differentiation between normal renal tissue and renal tumours using functional optical coherence tomography: A phase I in vivo human study," *BJU Int.* **110**, E415–E420 (2012).
18. S. Yazdanfar, A. M. Rollins, J. A. Izatt, "Imaging and velocimetry of the human retinal circulation with color Doppler optical coherence tomography," *Opt. Lett.* **25**(19), 1448–1450 (2000).
19. R. A. Leitgeb, L. Schmetterer, W. Drexler, A. F. Fercher, R. J. Zawadzki, T. Bajraszewski, "Real-time assessment of retinal blood flow with ultrafast acquisition by color Doppler Fourier domain optical coherence tomography," *Opt. Express* **11**(23), 3116–3121 (2003).
20. B. R. White, M. C. Pierce, N. Nassif, B. Cense, B. H. Park, G. J. Tearney, B. E. Bouma, T. C. Chen, J. F. de Boer, "In vivo dynamic human retinal blood flow imaging using ultra-high-speed spectral domain optical Doppler tomography," *Opt. Express* **11**(25), 3490–3497 (2003).
21. Y. Wang, A. Lu, J. Gil-Flamer, O. Tan, J. A. Izatt, D. Huang, "Measurement of total blood flow in the normal human retina using Doppler Fourier-domain optical coherence tomography," *Br. J. Ophthalmol.* **93**(5), 634–637 (2009).
22. L. An, R. K. Wang, "In vivo volumetric imaging of vascular perfusion within human retina and choroids with optical micro-angiography," *Opt. Express* **16**(15), 11438–11452 (2008).
23. Y. Wang, B. A. Bower, J. A. Izatt, O. Tan, D. Huang, "In vivo total retinal blood flow measurement by Fourier domain Doppler optical coherence tomography," *J. Biomed. Opt.* **12**(4), 041215 (2007).
24. R. Michaely, A. H. Bachmann, M. L. Villiger, C. Blatter, T. Lasser, R. A. Leitgeb, "Vectorial reconstruction of retinal blood flow in three dimensions measured with high resolution resonant Doppler Fourier domain optical coherence tomography," *J. Biomed. Opt.* **12**(4), 041213 (2007).
25. Z. Chen, T. E. Milner, S. Srinivas, X. Wang, A. Malekafzali, M. J. C. van Gemert, J. S. Nelson, "Noninvasive imaging of in vivo blood flow velocity

- using optical Doppler tomography,” *Opt. Lett.* **22**(14), 1119–1121 (1997).
26. Y. Zhao, Z. Chen, C. Saxer, S. Xiang, J. F. de Boer, J. S. Nelson, “Phase-resolved optical coherence tomography and optical Doppler tomography for imaging blood flow in human skin with fast scanning speed and high velocity sensitivity,” *Opt. Lett.* **25**(2), 114–116 (2000).
  27. J. Kehlet Barton, J. A. Izatt, M. D. Kulkarni, S. Yazdanfar, A. J. Welch, “Three-dimensional reconstruction of blood vessels from in vivo color Doppler optical coherence tomography images,” *Dermatology* **198**(4), 355–361 (1999).
  28. Y. Satomura, J. Seki, Y. Ooi, T. Yanagida, A. Seiyama, “In vivo imaging of the rat cerebral microvessels with optical coherence tomography,” *Clin. Hemorheol. Microcirc.* **31**(1), 31–40 (2004).
  29. Z. Luo, Z. Wang, Z. Yuan, C. Du, Y. Pan, “Optical coherence Doppler tomography quantifies laser speckle contrast imaging for blood flow imaging in the rat cerebral cortex,” *Opt. Lett.* **33**(10), 1156–1158 (2008).
  30. V. X. Yang, S. J. Tang, M. L. Gordon, B. Qi, G. Gardiner, M. Cirocco, P. Kortan, G. B. Haber, G. Kandel, I. A. Vitkin, B. C. Wilson, N. E. Marcon, “Endoscopic Doppler optical coherence tomography in the human GI tract: Initial experience,” *Gastrointest. Endosc.* **61**(7), 879–890 (2005).
  31. B. J. Vakoc, M. Shishko, S. H. Yun, W. Y. Oh, M. J. Suter, A. E. Desjardins, J. A. Evans, N. S. Nishioka, G. J. Tearney, B. E. Bouma, “Comprehensive esophageal microscopy by using optical frequency-domain imaging (with video),” *Gastrointest. Endosc.* **65**(6), 898–905 (2007).
  32. V. Jayaraman, J. Jiang, H. Li, P. J. S. Heim, G. D. Cole, B. Potsaid, J. G. Fujimoto, A. Cable, OCT Imaging up to 760 kHz Axial Scan Rate using Single-Mode 1310 nm MEMS-Tunable VCSELs with > 100 nm Tuning Range, in *Conf. Lasers and Electro-Optics: Applications and Technology*, p. PDPB2. Optical Society of America: Baltimore, MD (2011).
  33. S. Moon, D. Y. Kim, “Ultra-high-speed optical coherence tomography with a stretched pulse super-continuum source,” *Opt. Express* **14**(24), 11575–11584 (2006).
  34. Y. Chen, A. D. Aguirre, P. Hsiung, S. W. Huang, H. Mashimo, J. M. Schmitt, J. G. Fujimoto, “Effects of axial resolution improvement on optical coherence tomography (OCT) imaging of gastrointestinal tissues,” *Opt. Express* **16**, 2469–2485 (2008).
  35. R. Hattori, Y. Ono, M. Kato, T. Komatsu, Y. Matsukawa, T. Yamamoto, “Direct visualization of cortical peritubular capillary of transplanted human kidney with reperfusion injury using a magnifying endoscopy,” *Transplantation* **79**(9), 1190–1194 (2005).
  36. M. G. Snoeijs, H. Vink, N. Voesten, M. H. Christiaans, J. W. Daemen, A. G. Peppelenbosch, J. H. Tordoir, C. J. Peutz-Kootstra, W. A. Buurman, G. W. Schurink, L. W. van Heurn, “Acute ischemic injury to the renal microvasculature in human kidney transplantation,” *Am. J. Physiol. Renal Physiol.* **299**(5), F1134–F1140 (2010).
  37. J. Verbese, M. Cooper, P. Andrews, R. Derek, P. Moody, Y. Chen, “Using non-invasive, real-time imaging technology to assess the status of donor kidneys,” *Am. J. Transplantation* **13**(S5), 307 (2013).